Available online at www.sciencedirect.com

SciVerse ScienceDirect

Ceramics International 39 (2013) 337–346

CERAMICS INTERNATIONAL

www.elsevier.com/locate/ceramint

Tool life and wear of WC–TiC–Co ultrafine cemented carbide during dry cutting of AISI H13 steel

Ji Xiong[a], Zhixing Guo[a,*], Mei Yang[b], Weicai Wan[a], Guangbiao Dong[a]

[a]School of Manufacturing Science and Engineering, Sichuan University, Chengdu 610065, P.R.China
[b]College of Materials and Chemistry & Chemical Engineering, Chengdu University of Technology, Chengdu 610059, P.R. China

Received 17 March 2012; received in revised form 9 June 2012; accepted 10 June 2012
Available online 16 June 2012

Abstract

WC–5TiC–10Co ultrafine cemented carbides were prepared and used for the cutting tool for AISI H13 hardened steel. The effect of cutting parameters on the tool life and tool wear mechanism was investigated, and conventional cemented carbide with the same composition and medium grain size were prepared for comparison. The results showed that WC–5TiC–10Co ultrafine cemented carbides possess higher hardness and transverse rupture strength, and showed better cutting performance than conventional insert with the same cutting condition. Tool life was analyzed by an extended Taylor's tool life equation, indicating that cutting speed played a profound effect on the tool life and wear behavior of both cutting inserts. SEM and EDS analysis revealed that there were major adhesive wear and minor abrasive wear on the rake of WC–5TiC–10Co ultrafine inserts, and increase of cutting speed resulted in a transition from abrasion predominant wear mechanism to adhesive wear on the flank face. As for the conventional inserts, there were combination of more serious abrasive and adhesive wear on the rake and flank. The favorable cutting performance of ultrafine WC–5TiC–10Co inserts was attributed to the higher hardness and less thermal softening during machining.

Keywords: A. Sintering; B. Grain size; C. Wear resistance; E. Cutting tools

1. Introduction

AISI H13 hardened steel possess high hardness, toughness, high temperature strength, high resistance to thermal shock, thermal fatigue and thermal softening. Therefore, it has been widely used as hot work dies such as die-casting dies, extrusion dies, hot forging dies and plastic mold dies [1]. Traditionally, dies/mold manufacturing process generally involves conventional machining in the annealed (soft) state followed by electro-discharge machining (EDM) and manual polish/finish grinding [2]. With the progress in machining and cutting technology, hard cutting and dry cutting are applied when higher demand of die quality, cost, effectiveness and environmental requirement are considered [3]. Due to the aggressive cutting condition and its mechanical properties, the hardened H13 steel is recognized to be a kind of difficult-to-cut material.

Cutting of H13 hardened steel has always been an important subject of many publications and received great attention. Ng and Aspinwall [4] investigated the effect of workpiece hardness and cutting speed on the machinability of AISI H13 hot work die steel using PCBN tooling. Cardoso et al. [5] carried out end milling of AISI H13 steels with (Ti,Al)N-coated and PCBN-tipped tools, and the temperature of workpiece was compared in terms of different cooling method. Ghani et al. [6] studied the performance of TiN-coated P10 carbide tools for end milling of AISI H13 steel at a higher cutting speed and the feed rate and depth of cut had the most significant effect on tool life. Elbestawi et al. [7] investigated the cutting tool performance and surface finish of hardened AISI H13 tool steel for different process parameters. Kovalev et al. [8] deposited $(Ti_{0.33}Al_{0.67})N$ and $(Ti_{0.1}Al_{0.7}Cr_{0.2})N$ coatings on WC–Co cemented carbide substrates, and the results showed that TiAlCrN coatings were preferable for the end milling of H13 (HRC 50–52) hardened tool steel. Ning et al. [9] investigated the wear

*Corresponding author. Tel.: +86 13688313720; fax: +86 28 85196764.
E-mail address: submission001@hotmail.com (Z. Guo).

0272-8842/$36.00 © 2012 Elsevier Ltd and Techna Group S.r.l. All rights reserved.
http://dx.doi.org/10.1016/j.ceramint.2012.06.031

behavior and chip formation during dry machining of AISI H13 hardened steel (HRC 55–57) using nano-multilayered TiAlCrN/NbN coated ultrafine grained cemented carbide. de Oliveira et al. [10] carried out several milling experiments on the AISI H13 steel with a hardness of 50 HRC using multiple layers of TiCN and TiN coated sandvik GC1025 cemented carbide tools. The influence of workpiece surface inclination and cutting conditions on tool life and tool wear mechanisms was investigated.

Generally, various cutting tool materials including PCBN, coated WC–Co ultrafine cemented carbides and *P* series cemented carbides were used for cutting of AISI H13 steel. However, hitherto, the cutting of AISI H13 hardened steel remains a big challenge. Therefore, development of high performance cutting tool materials with the combination of hardness and toughness are strongly necessary for AISI H13 hardened steel cutting. It is well known that high performance hard materials can be achieved by preparation of ultrafine WC–Co cemented carbides (ISO K series) [11–17], which has been used as micro-drills for printed circuit board (PCB), wear-resistant parts and metal cutting tools [18,19]. However, the refinement of cemented carbides has not been applied to WC–TiC–Co cemented carbides (ISO P series) [20], which are more widely used as steel cutting tools than WC–Co cemented carbides.

In the paper, ISO P series WC–5TiC–10Co ultrafine cemented carbides were prepared. The microstructure and mechanical properties of the ultrafine cemented carbides were characterized and used for AISI H13 hardened steel cutting. The effect of cutting parameters including feed rate, cutting speed and depth of cut on the flank wear were measured, the tool life were evaluated by extended Taylor's equation and the wear morphology of the inserts were observed and analyzed. To the best of the authors' knowledge, little been reported about WC–TiC–Co ultrafine cemented carbides and its performance during ANSI H13 steel cutting. Conventional cemented carbides with the same composition of WC–5 wt%TiC–10 wt%Co but coarser grain size were employed throughout the research for comparison.

2. Experimental procedures

2.1. Preparation and characterization of WC–5TiC–10Co cemented carbides inserts

Commercially available ultrafine WC, ultrafine Co, micro-scaled (W,Ti)C solid solution and nano TiC powders were used as raw materials, and ultrafine W powder was used to achieve carbon balance. Characteristics of these powders were listed in Table 1. Firstly, the micro-scaled (W,Ti)C solid solution powder was pre-ball milled for 72 h and the nano TiC powder was ultrasonic dispersed aided by Tween 80 addition, and the processing details were discussed elsewhere [21], other raw powders were used without further treatment. Ultrafine WC–5 wt% TiC-–10 wt%Co cemented carbides were prepared according to normal powder metallurgical procedures. The powders were ball milled in ethanol in stainless steel lined mills for 72 h. WC–6 wt%Co ultrafine cemented carbide balls with a diameter of 6 mm were used as the milling bodies, the ball to powder weight ratio was selected to be 10:1, and the milling speed was 56 r/min. After milling the pulp was vacuum-dried, synthetic rubber was added as the pressing aid. Rectangular specimens of a dimension of 6.5 mm × 5.25 mm × 20 mm were pressed for transverse rupture strength test, and T31605F type inserts were pressed for cutting performance test. The pressed pieces (green bodies) were sintered in vacuum furnace of pilot scale at 1410° for 1.5 h to form the final geometry. Conventional cemented carbides with the same composition of WC–5 wt%TiC–10 wt%Co but coarser grain size were prepared using 6.0 μm WC, and used for cutting performance comparison. S-4800 scanning electron microscope (SEM) (Hitachi, Japan) and CK40M optical microscopy (Olympus, Japan) were used for microstructure observation. Transverse rupture strength test was performed using WE-100B universal material testing machine (Changchun testing machine plant, China), coercive force and magnetic saturation were tested by YSK-III and MCoM-3 instruments (Hunan, China), hardness was measured using ARK-600 Rockwell hardness

Table 1
Characteristics of various raw materials.

Raw materials		WC	(W,Ti)C	Co	W	TiC
Fisher sub-sieve sizer (μm)		0.4–0.5	2.47	0.4	0.4	0.05
Brunauer Emmett Teller specific surface area (m^2/g)		2.53	0.089	2.0	4.0	23
Chemical composition (wt%)	Total carbon	6.19	9.80	0.024	0.002	19.21
	O	0.29	0.086	0.6	0.10	0.20
	Ti	/	24.12	/	/	bal
	Co	/	/	bal	/	/
	VC	0.33	/	/	/	/
	W	bal	bal	/	bal	/
	Cr_3C_2	0.90	/	/	/	/
Manufacturer		Xiamen Golden Egret Special Alloy Co. Ltd, China				Hefei Kaier Nanometer Energy & Technology Co. Ltd, China

tester(AKashi, Japan), and density was measured using BS224S balance (Satorius, 0.0001 mg sensitive quantity, China) by Archimedes method.

2.2. Cutting performance test

The sintered T31605F inserts cemented carbides were grinded for continuous turning tests. The shape and size of T31605F inserts was shown in Fig. 1. The inserts were clamped to a commercial tool holder. Combination of the insert and the tool holder resulted in a rake angle of 8° and clearance angle of 8°. Workpieces was a ∅40 mm cylinder AISI H13 hot work die steel, which had a hardness of 50 HRC after quenching and tempering process. Table 2

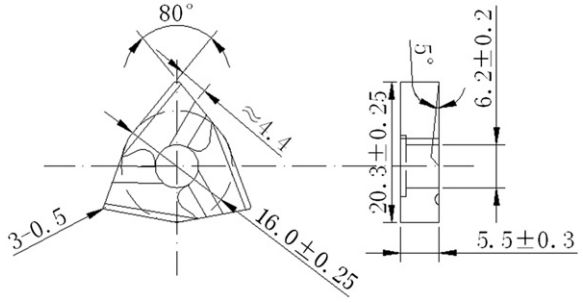

Fig. 1. Schematic of T31605F type insert.

Table 2
Cutting performance test details for ultrafine and conventional WC–5TiC–10Co cemented carbide inserts.

Group	Experiment number	*f* (mm/r)	*ap* (mm)	*Vc* (m/min)
I	1	0.159	0.2	120
	2	0.396	0.2	120
	3	0.521	0.2	120
II	1	0.159	0.2	120
	4	0.159	0.2	152
	5	0.159	0.2	176
III	1	0.159	0.2	120
	6	0.159	0.4	120
	7	0.159	0.6	120

showed the cutting conditions, in which the cutting performance tests were divided into three groups and the feed rate, cutting speed and depth of cut were changed. Continuous turning tests were conducted using a CD6140A turning lathe (Chongqing no. 2 Machine Tool Works, China), and no cutting fluid was applied. For a single cutting parameters combination, the cutting test was repeated three times using the three cutting edges of the indexable T31605F insert. A new cutting edge was used for each test. The flank wear was measured by toolmaker's microscope every 2 min of cutting. Flank wear VB_B value of 0.3 mm was used as the tool life criterion for the continuous turning operations according to ISO standard 3685. Tool life was considered ended when flank wear reached VB_B=0.30 mm. After the end of tool life, worn surfaces of the cemented carbide inserts were ultrasonically cleaned with acetone, and S-4800 scanning electron microscope (SEM) equipped with an energy dispersive X-ray spectrometer (EDS) was used to examine the nature of the worn rake and flank faces in an attempt to understand the wear mechanisms. For the sake of comparison, the cutting tests were also carried out using conventional cemented carbide inserts.

3. Results and discussion

3.1. Microstructure and properties of inserts

Fig. 2 showed the SEM images of both the WC–5TiC–10Co ultrafine and conventional cemented carbides inserts. When observed by SEM in BSE mode, element with larger atom number shows lighter color [22]. The WC grains appeared white with prismatic angles, and (W,Ti)C solid solution grains were black with irregular shape. It can be seen that both the WC and the solid solution phases of ultrafine cemented carbide had a grain size of approximate 0.5 μm. However, the conventional cemented carbide showed an average WC grain size of 1.8 to 2.4 μm and an average solid solution grain size of 1.0 to 1.5 μm. The distinct microstructure differences largely affect the properties and cutting performance of the cemented

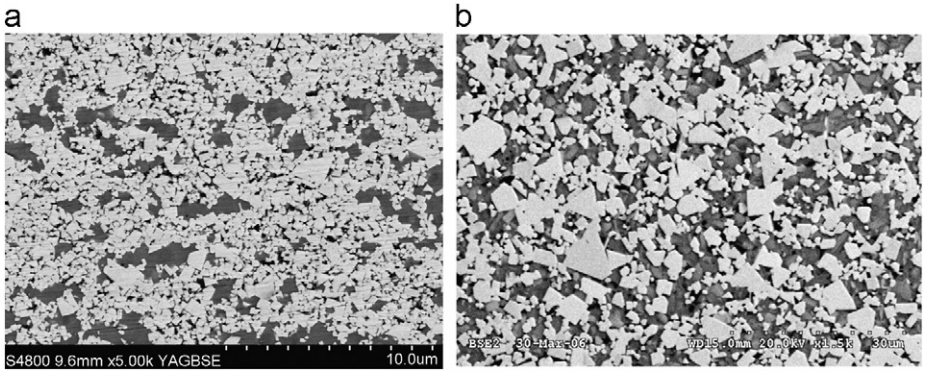

Fig. 2. SEM images of both cemented carbide inserts. (a) Ultrafine and (b) conventional.

Table 3
Low magnification microstructure and mechanical properties of both cemented carbides.

Inserts	Ultrafine	Conventional
Low magnification microstructures	A02B00C00	A02B00C00
Density (g/cm^3)	13.15	13.17
Hardness (HRA)	93.0	90.8
Coercive force (kA/m)	31.78	13
Relative maganet saturation (%)	9.12	9.25
Transverse rupture strength (MPa)	2392	2087
α phase grain size (μm)	0.5–0.6	1.8–2.4
β phase grain size (μm)	0.5–0.6	<1.5

carbides inserts.Low magnification microstructures and mechanical properties of both inserts were listed in Table 3. According to the ISO norm 4505, pores smaller than 10 μm are designated "A" pores and those larger than 10 μm but smaller than 25 μm are called "B" pores [23]. The polished samples of both inserts showed only type A porosity with a concentration of A02, hence, WC–5TiC–Co inserts with full density were achieved. Both inserts showed similar density due to the same nominal chemical composition and low magnification microstructures. The coercive force is believed to increase with decreasing hard phase grain size and the distribution of binder phase. The magnetic saturation is sensitive to the carbon content of the system and an indirect measurement of the solution hardening of the binder phase. Though both inserts showed similar relative magnetic saturation, ultrafine inserts had a much larger coercive force of 31.78 kA/m than 13.00 kA/m of conventional inserts due to the ultrafine grain size. With the decrease of grain size, especial to ultrafine scope, the transverse rupture strength increased along with the hardness according to Hall–Petch formula. The WC–5TiC–10Co ultrafine cemented carbide showed larger transverse rupture strength of 2392 MPa and hardness of 93.0HRA. Generally, WC–5TiC–10Co ultrafine cemented carbides possessed better mechanical properties than conventional inserts of the same composition.

3.2. Tool life

During machining, instead of catastrophic tool failure, tool life can be defined in terms of the progressive wear which occurs on the tool rake face and/or clearance face, i.e. crater wear and flank wear. Flank wear is used to characterize the tool life, which has a major negative influence on the on dimensional accuracy and surface finish of the component as well as the stability of the machining process when the flank wear land width VB_B value reach a certain level [24]. Hence, the paper concentrates on the flank wear and tool life when machining with both cemented carbide inserts.

The flank wear VB_B values of both cemented carbide inserts were measured and the average values were plotted as a function of cutting time with different values of feed rate, cutting speed and depth of cut, which were shown in Figs. 3–5, respectively. It is noted that larger feed rate, cutting speed and depth of cut mean serious thermal, mechanical and chemical impact on the cutting tool. Therefore, it can be concluded that after turning of the AISI H13 cylinder workpieces, the flank wear VB_B values of both inserts increased with every cutting parameter. Classical tool wear process can be seen is all the figures, which contain three stages including rapid initial wear followed by gradual or little wear and finally rapid or catastrophic wear [25]. Generally, the WC–5TiC–10Co ultrafine cemented carbide insert showed less serious flank wear than conventional insert.

Tool life can be characterized by the working time of insert without adjustment or replacement, the number of parts machined, the length of the tool path or the area of the machined surface [26]. In the paper, the tool life has been defined as the elapsed machining time when the flank wear reaches the allowed limit equal to the criterion 0.3 mm. The calculated average values and the standard

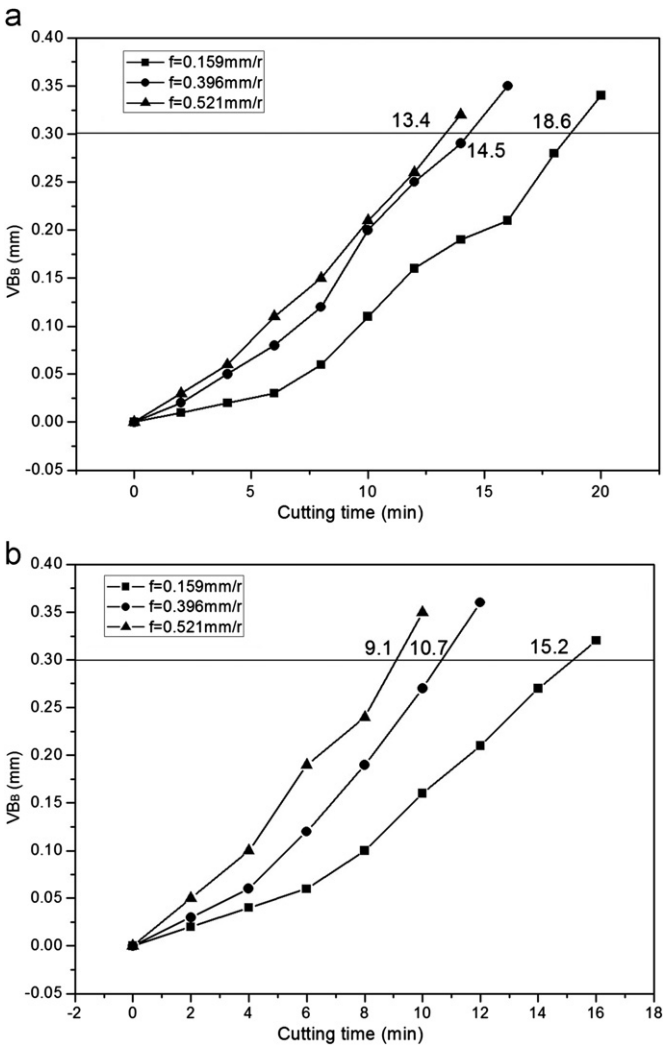

Fig. 3. Flank wear VB_B values as a function of cutting time of both cemented carbides inserts with different feed rate. (a) Ultrafine insert and (b) conventional insert.

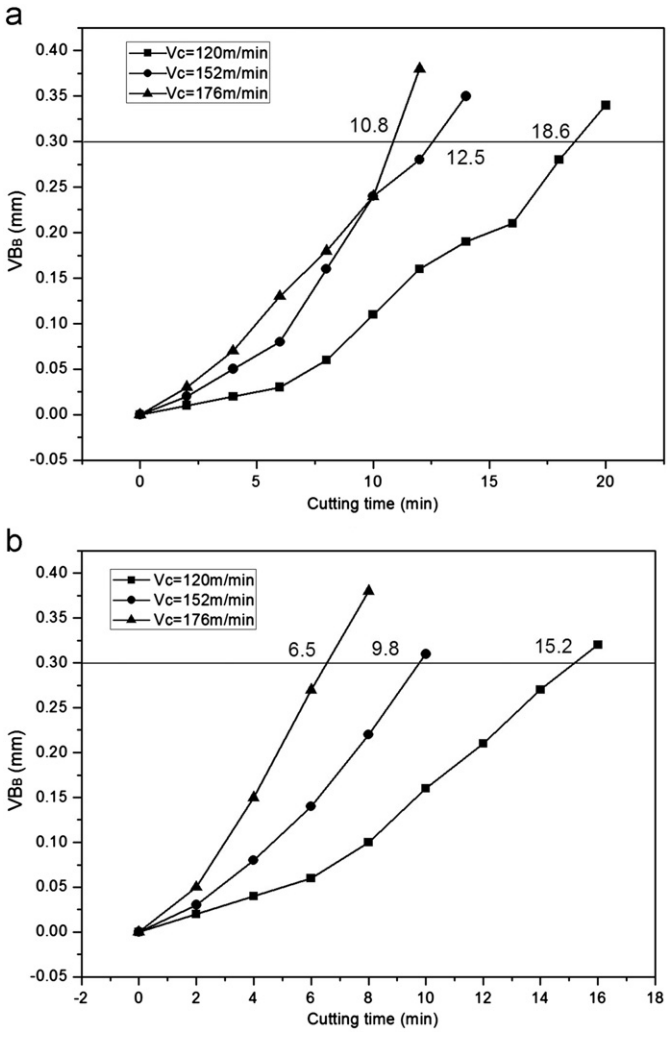

Fig. 4. Flank wear VB_B values as a function of cutting time of both cemented carbides inserts with different cutting speed. (a) Ultrafine insert and (b) conventional insert.

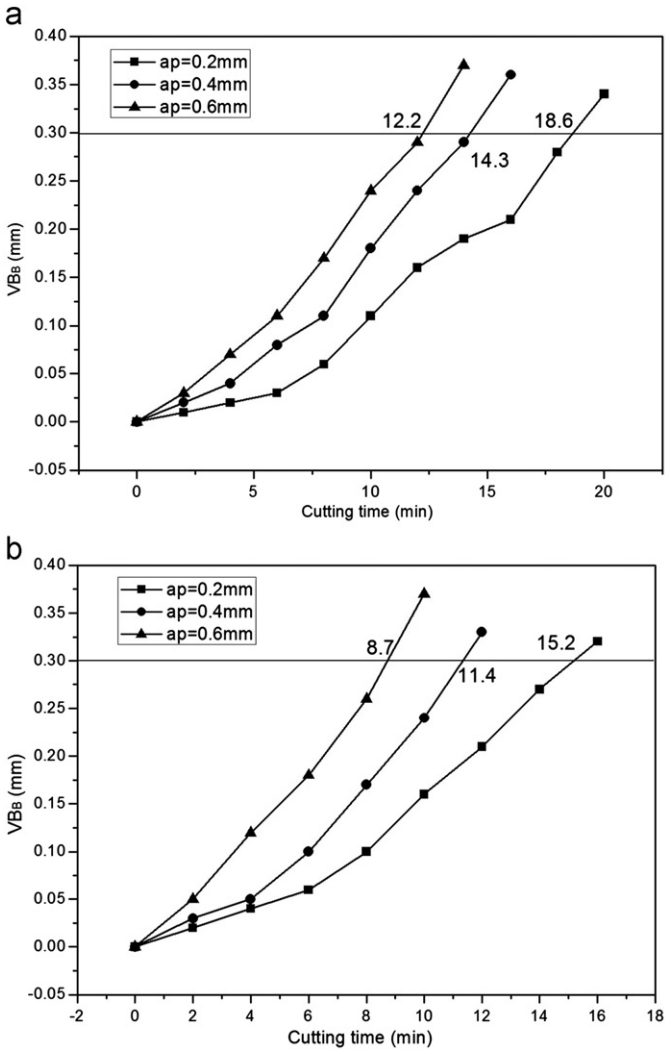

Fig. 5. Flank wear VB_B values as a function of cutting time of both cemented carbides inserts with different depth of cut. (a) Ultrafine insert and (b) conventional insert.

deviations of tool life of both inserts with different cutting parameters were listed Table 4. Tool life decreased with the cutting parameters, and the ultrafine inserts had longer tool life than conventional inserts.

Although various forms of equations were developed to relating tool life to the main machining parameters involved, the tool life equation derived by F. W. Taylor was undoubtedly the most famous one. Initially, only the cutting speed *Vc* was considered as the main factor. Later, other parameters such as feed rate *f* and depth of cut *ap* were taken into account and the Taylor's tool life equation was extended to the form shown in Eq. (1) as follows [27]:

$$T = \frac{C_T}{V_c^{1/m} f^{1/n} a_p^{1/p}} \quad (1)$$

where T is the tool life ($_{\min}$), Vc is the cutting speed (m/min), f is the feed rate ($_{\min}$/r), ap is the depth of cut (mm), C_T is the tool life constant which corresponds to the workpiece materials, cutting inserts and other cutting conditions, the Taylor exponents factor m, n, p indicating the effect of the cutting parameters.

Table 4
The tool life of both inserts with different cutting parameters.

f (mm/r)	*ap* (mm)	*Vc* (m/min)	Tool life of conventional insert ($_{\min}$)		Tool life of ultrafine insert ($_{\min}$)	
			Average	Standard deviation	Average	Standard deviation
0.159	0.2	120	15.2	0.08	18.6	0.09
0.396	0.2	120	10.7	0.06	14.5	0,07
0.521	0.2	120	9.1	0.04	13.4	0.07
0.159	0.2	120	15.2	0.08	18.6	0.09
0.159	0.2	152	9.8	0.07	12.5	0.07
0.159	0.2	176	6.5	0.04	10.8	0.04
0.159	0.2	120	15.2	0.08	18.6	0.09
0.159	0.4	120	11.4	0.08	14.3	0.07
0.159	0.6	120	8.7	0.04	12.2	0.05

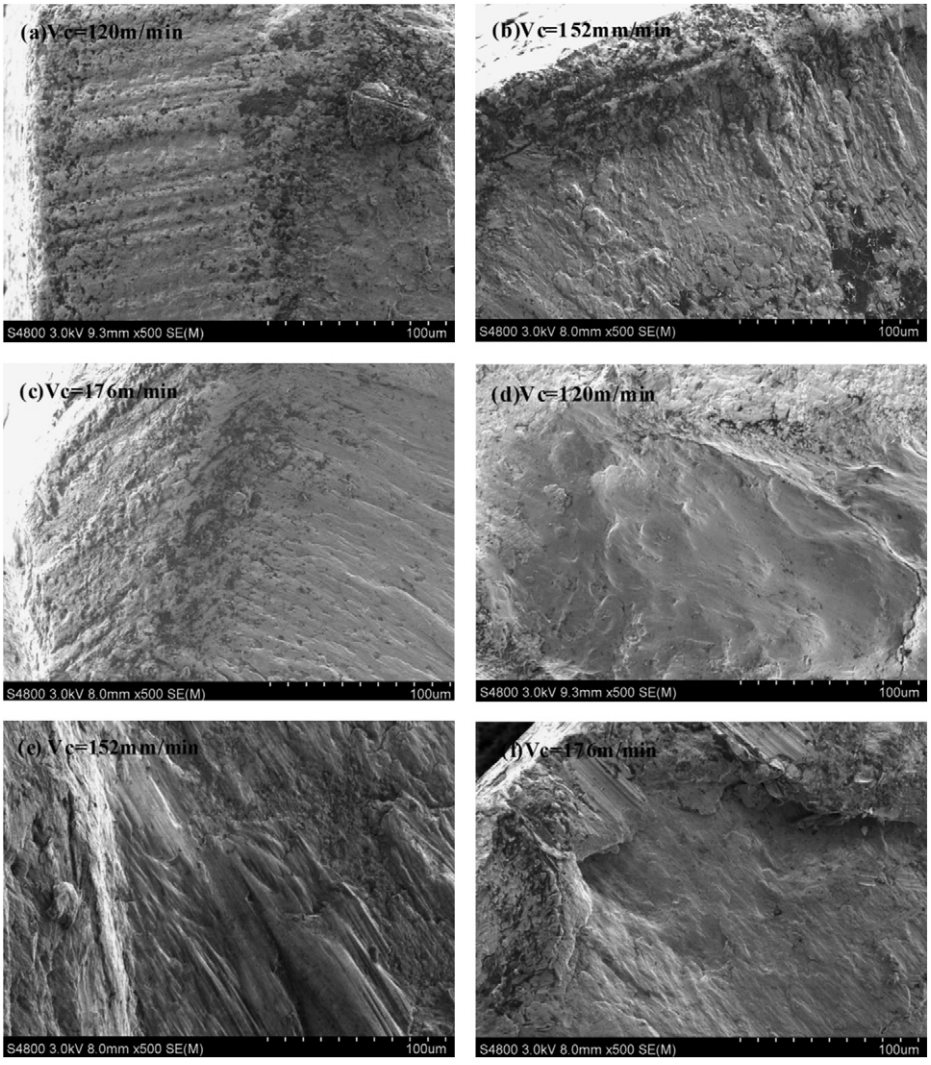

Fig. 6. The rake wear morphology of both ultrafine (a,b,c) and conventional (d,e,f) cemented carbide inserts machined with different cutting speed shown in the top left of each figure.

The multiple nonlinear regression method was used for estimation of the Taylor coefficients. The achieved Taylor's equations of ultrafine and conventional inserts were given in Eqs. (2) and (3).

$$T_{ultrafine} = \frac{7.208 \times 10^3}{V_c^{1/0.677} f^{1/3.698} a_p^{1/2.650}} = \frac{7.208 \times 10^3}{V_c^{1.477} f^{0.270} a_p^{0.377}} \quad (2)$$

$$T_{conventional} = \frac{9.900 \times 10^4}{V_c^{1/0.462} f^{1/2.335} a_p^{1/2.013}} = \frac{9.900 \times 10^4}{V_c^{2.164} f^{0.428} a_p^{0.496}} \quad (3)$$

The calculated tool life agreed well with the experiment results (The R values of the above regression results were 0.997 and 0.995, respectively). It can be seen that cutting speed Vc played a predominant role in determining the tool performance in terms of tool life, followed by depth of cut and feed rate. Both inserts showed similar tendency, and all Taylor exponent values increased with the grain size of the inserts. Not only the tool life can be estimated by the extended Taylor's equation, but also optimal cutting parameters can be achieved. As for the cutting of AISI H13 steel, relative large feed rate and depth of cut can be selected, and cutting speed should be determined according to the cutting efficiency, workpiece surface integrity and tool endurance. The cutting parameters Vc = 120 mm/min, ap = 0.2 mm, f = 0.521 mm/r can be used for reference.

3.3. Tool wear

From Section 3.2, the cutting speed Vc was the major cutting parameter which influenced the tool life mostly. Therefore, SEM and EDS were used for the investigation of all worn inserts machining with different cutting speed. During the cutting test, the depth of cut ap and feed rate f were kept constant at 0.2 mm and 0.159 mm/r, respectively, and the cutting speed Vc varied at 120, 152 and 176 m/min. While machining AISI H13 hardened steel, the contact friction between the tool–workpiece and tool–chip

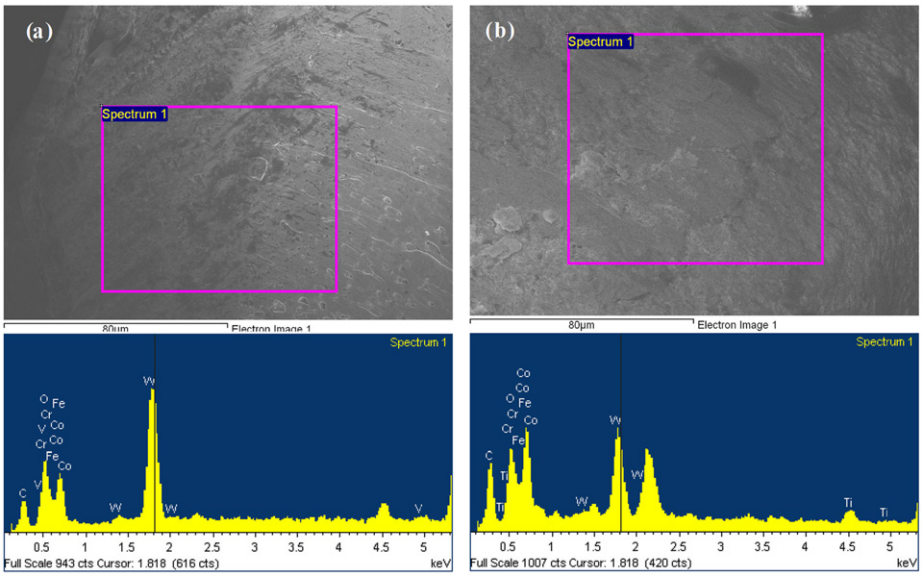

Fig. 7. EDS spectrum of the worn rake face of both inserts when cutting test finished at the cutting speed of 176 mm/r. (a) Ultrafine insert and (b) conventional insert.

interfaces generated high temperatures on the cutting tool. Two main types of tool wear gradually occurred on the top rake face and the flank, i.e. crater wear and flank wear. Crater wear was formed due to the sliding of the chips against the rake surface, and the flank wear resulted from the friction between the newly generated workpieces surface and the flank face adjacent to the cutting edge [28].

The rake wear morphologies of both ultrafine and conventional cemented carbide inserts were shown in Fig. 6. As for the ultrafine insert, there was adhesive wear on the rake face when the cutting test finished with a cutting speed of 120 m/min. With the increase of cutting speed increased to 152 m/min, the adhesive wear became obvious, especially in the chip breaker groove. With the increase of cutting speed increased to 176 m/min, the adhesive wear appeared more serious, and scratches can also be seen on the adhesive layer of the rake face due to the high speed flow of chips. As for the conventional inserts, crater wear can be seen on the rake, which indicated more serious wear during the cutting of H13 hardened tool steel with high strength and hardness. With the increase of cutting speed increased to 152 m/min, the adhesive layer was thicker and deep scratches remained when the chips passed away. With the increase of cutting speed increased to 176 m/min, there was amazing rake wear, and even the tool materials spalling after the adhesive of workpiece materials can be seen on the rake face.

Fig. 7 showed the EDS spectrum of the worn rake faces of both inserts when cutting test finished at the cutting speed of 176 mm/r. Fe, Cr, Co and W content can be seen on the worn rake faces of both inserts. The existence of Fe and Cr elements indicated the adhesion of AISI H13 workpiece materials on the tool insert due to the pressure and heat produced during cutting process. The existence of W and Co elements indicated the abrasive wear between the cutting chips and the tool materials. There were Fe, Cr, Co and W peaks on the worn rake area of both insert, revealing a combination of adhesive wear abrasive wear. Considering the wear morphology and EDS peaks intensity, it can be concluded that there was major abrasive wear and minor adhesive wear on the rake of ultrafine inserts, and combination of more serious adhesive and abrasive wear on the rake of conventional inserts.

The flank wear morphologies of both ultrafine and conventional cemented carbide inserts were shown in Fig. 8. As for the ultrafine insert, abrasive wear can be seen on the flank face when the cutting test finished with a cutting speed of 120 m/min. It can be concluded that though the hardness of the cemented carbide was largely improved due to refinement of the grains, the oxide and carbide particles of high hardness generated during the cutting of AISI H13 hardened steel will result in the aggravation of tool wear. With the increase of cutting speed increased to 152 m/min, obvious adhesive wear and cutting edge micro-blasting can be observed. With the increase of cutting speed increased to 176 m/min, the abrasive wear changed to adhesive wear totally. As for the conventional inserts, serious adhesive wear can be seen and even spalling. With the increase of cutting speed increased to 152 m/min, there can be seen thick adhesive of workpieces materials, indicating amazing adhesive wear. With the increase of cutting speed increased to 176 m/min, the cutting force increase accordingly, and the cutting inserts breakage occurred due to the relatively lower properties of conventional inserts.

Fig. 9 showed the EDS spectrum of the worn flank faces of both inserts when cutting test finished at the cutting speed of 176 mm/r. As for the ultrafine inserts, there existed intensive W and Fe peaks, compared to the

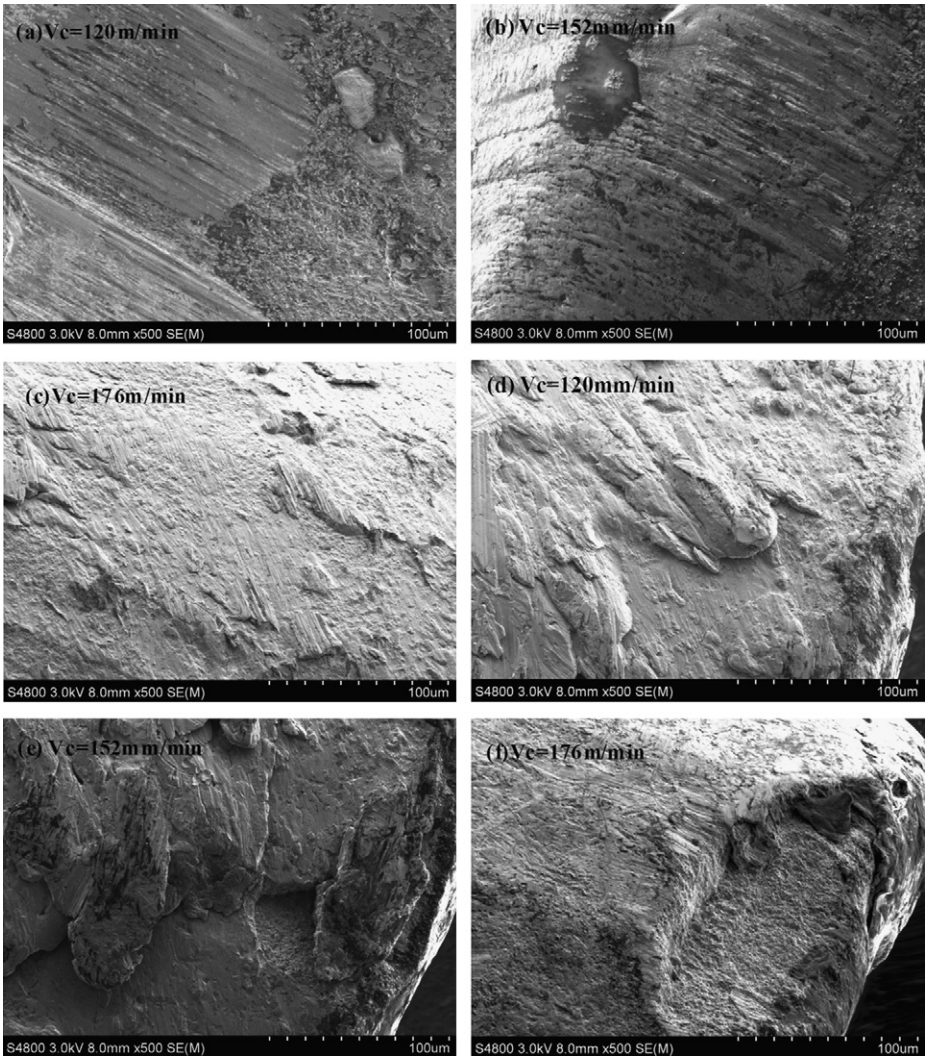

Fig. 8. The flank wear morphology of both ultrafine (a,b,c) and conventional (d,e,f) cemented carbide inserts machined with different cutting speed shown in the top left of each figure.

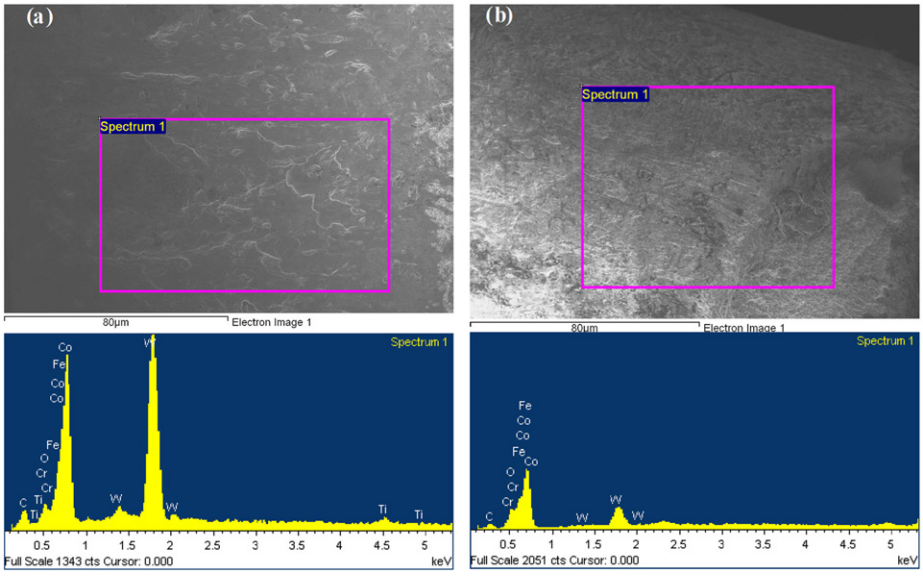

Fig. 9. EDS spectrum of the worn flank face of both inserts when cutting test finished at the cutting speed of 176 mm/r. (a) Ultrafine insert and (b) conventional insert.

conventional insert. The EDS spectrum showed fewer Fe and Cr content in the conventional insert due to the breakage of the cutting edge at an early time. Generally, it is well accepted that several wear mechanisms such as abrasion, adhesion, oxidation, diffusion can operate simultaneously during machining [29]. During cutting of AISI H13 hardened steel, Abrasive wear occurs when escaped hard particles from workpieces and tools move across the contact area. With the increase of cutting speed, adhesion of the tool and workpiece increases at higher temperatures, and tool flank adhered to the workpiece surface are periodically sheared off. There was serious adhesive wear and even spalling of tool materials on the flank surface, the spalling will result in the sudden decrease of the contact areas between the flank and workpiece, then the cutting stress on the spalling area will increase accordingly, and the wear will become more serious. Simultaneously, the spalled tool materials will act as the third body abrasive particles and result in aggressive abrasive wear. With the increase of cutting speed, the extrusion deformation effect increase. The cutting inserts experience a course of microcrack formation, combination, spread and sudden failure finally with the double impact of heat and force. The flank wear of conventional insert showed serious adhesive wear and breakage of cutting edge finally took place with high cutting speed. As for the ultrafine insert, there were less serious flank wear which changed from abrasive wear to adhesive wear with the increase of cutting speed.

Generally, during dry cutting of AISI H13 hardened steel, thermal and mechanical impact on the tool increase with cutting speed. For cutting edge temperatures below 700–800°,the high hardness and yet more pronounced red hardness, thermal wear resistance and cutting edge stability of WC–5TiC–10Co ultrafine inserts resulted in longer life time and allow higher cutting speeds compared to conventional inserts[18]. There existed less serious crater wear and flank wear of ultrafine inserts.

4. Conclusions

(1) WC–5TiC–Co ultrafine cemented carbides were prepared and used for AISI H13 hardened steel cutting tool. The ultrafine inserts have a low magnification microstructure of A02B00C00 with ultrafine WC and (W,Ti)C solid solution grains. The ultrafine inserts showed higher hardness and transverse rupture strength of 93.0HRA and 2392 MPa, compared to 90.8HRA and 2087 MPa of conventional insert.

(2) Cutting performance test were carried out using both ultrafine and conventional WC–5TiC–Co inserts. Flank wear was measured as a function of cutting time with different cutting parameters. The WC–5TiC–10Co ultrafine cemented carbide insert showed less serious flank wear than conventional insert. Tool life was estimated by extended Taylor's equation, indicating that cutting speed played a profound role in the wear behavior of both inserts during H13 steel cutting.

(3) SEM and EDS were used for worn rake and flank face investigation. There was slight adhesive and abrasive wear on the rake of ultrafine insert, and more serious combination of the above wear patterns as for conventional insert. With the increase of cutting speed, there was a transition from abrasion predominant wear mechanism to adhesive wear on the flank face of ultrafine insert. As for the conventional insert, there existed amazing adhesive wear on the flank and edge breakage occurred at large cutting speed. The favorable of the WC–5TiC–10Co ultrafine inserts can be attributed to the refinement of grains and excellent mechanical properties.

Acknowledgments

The study is financially supported by Research Funds for the Central Universities (no. 2011SCU11038) and Chengdu Science and technology Project (no. 10GGZD080GX-268 and 11DXYB096JH-027). The authors are grateful to Chengdu Mingwu Technology Corp., Ltd. of China for supply of materials. Thanks are also extended to Analytical & Testing Center of Sichuan University for the testing of the samples.

References

[1] H. Yan, J. Hua, R. Shivpuri, Flow stress of AISI H13 die steel in hard machining, Materials and Design 28 (2007) 272–277.
[2] D.A. Axinte, R.C. Dewes, Surface integrity of hot work tool steel after high speed milling-experimental data and empirical models, Journal of Materials Processing Technology 127 (2002) 325–335.
[3] H.K. Tonshoff, C. Arendt, A.R. Ben, Cutting of hardened steel, CIRP Annals—Manufacturing Technology 49 (2000) 547–566.
[4] E. Ng, D.K. Aspinwall, The effect of workpiece hardness and cutting speed on the machinability of AISI H13 hot work die steel when using PCBN tooling, Journal of Manufacturing Science and Engineering 124 (2002) 582–594.
[5] B.L. Cardoso, C.R. Teixeira, R.A. Roger, Experimental and theoretical study of work piece temperature when end milling hardened steels using TiAlN coated & PCBN-tipped tools, Journal of Materials Processing Technology 199 (2008) 234–244.
[6] J.A. Ghani, I.A. Choudhury, H.H. Majuki, Performance of P10 TiN coated carbide tools when end milling AISI H13 tool steel at highcutting speed, Journal of Materials Processing Technology 154 (2004) 1062–1066.
[7] M.A. Elbestawi, L. Chen, C.E. Becze, T.I. El-Wardany, High speed milling of dies and moulds in their hardened state, CIRP Annals—Manufacturing Technology 46 (1997) 57–62.
[8] A.I. Kovalev, D.L. Wainstein, A.Y. Rashkovskiy, G.S. Fox-Rabinovich, K. Yamamoto, S. Veldhuis, M. Aguirre, B.D. Beake, Impact of Al and Cr alloying in TiN-based PVD coatings on cutting performance during machining of hard to cut materials, Vacuum 84 (2010) 184–187.
[9] L. Ning, S.C. Veldhuis, K. Yamamoto, Investigation of wear behavior and chip formation for cutting tools with nano-multilayered TiAlCrN/NbN PVD coating, International Journal of Machine Tools 48 (2008) 656–665.
[10] A.J. de Oliveiraa, A.E. Diniz, Tool life and tool wear in the semi-finish milling of inclined surfaces, Journal of Materials Processing Technology 209 (2009) 5448–5455.

[11] N.G. Hashe, J.H. Neethling, P.R. Berndt, H.O. Andrén, S. Norgren, A comparison of the microstructures of WC–VC–TiC–Co and WC–VC–Co cemented carbides, International Journal of Refractory Metals & Hard Materials 25 (2007) 207–213.
[12] V. Bonache, M.D. Salvador, V.G. Rocha, A. Borrell, Microstructural control of ultrafine and nanocrystalline WC–12Co–VC/Cr_3C_2 mixture by spark plasma sintering, Ceramics International 37 (2011) 1139–1142.
[13] H.C. Kim, I.J. Shon, J.K. Yoon, J.M. Doh, Consolidation of ultra fine WC and WC–Co hard materials by pulsed current activated sintering and its mechanical properties, International Journal of Refractory Metals & Hard Materials 25 (2007) 46–52.
[14] I.C. Seung, H.H. Soon, B.K. Kim, Spark plasma sintering behavior of nanocrystalline WC-10Co cemented carbide powders, Materials Science & Engineering A—Structural Materials 351 (2003) 31–38.
[15] E. Breval, J.P. Cheng, D.K. Agarwal, P. Gigl, M. Dennis, R. Roy, A.J. Papworth, Comparison between microwave and conventional sintering of WC/Co composites, Materials Science & Engineering A—Structural Materials 391 (2005) 285–295.
[16] D.H. Xiao, Y.H. He, M. Song, N. Lin, R.F. Zhang, Y_2O_3- and NbC-doped ultrafine WC–10Co alloys by low pressure sintering, International Journal of Refractory Metals & Hard Materials 28 (2010) 407–411.
[17] A. Delanoe, M. Bacia, E. Pauty, S. Lay, C.H. Allibert, Cr-rich layer at the WC/Co interface in Cr-doped WC–Co cermets: segregation or metastable carbide, Journal of Crystal Growth 270 (2004) 219–227.
[18] G. Gille, B. Szesny, K. Dreyer, H. van den Berg, J. Schmidt, T. Gestrich, G. Leitner, Submicron and ultrafine grained hardmetals for microdrills and metal cutting inserts, International Journal of Refractory Metals & Hard Materials 20 (2002) 3–22.
[19] D.H. Xiao, Y.H. He, W.H. Luo, M. Song, Effect of VC and NbC additions on microstructure and properties of ultrafine WC–10Co cemented carbides, Transactions of Nonferrous Metals Society 19 (2009) 1520–1525.
[20] K.H. Lee, S.I. Cha, B.K. Kim, S.H. Hong, Effect of WC/TiC grain size ratio on microstructure and mechanical properties of WC–TiC–Co cemented carbides, International Journal of Refractory Metals & Hard Materials 24 (2006) 109–114.
[21] Z.X. Guo, J. Xiong, M. Yang, S.J. Xiong, J.Z. Chen, Y.M. Wu, H.Y. Fan, L. Sun, J. Wang, H. Wang, Dispersion of nano-TiN powder in aqueous media, Journal of Alloys and Compounds 493 (2010) 362–367.
[22] Z.X. Guo, J. Xiong, M. Yang, X.Y. Song, C.J. Jiang, Effect of Mo_2C on the microstructure and properties of WC–TiC–Ni cemented carbide, International Journal of Refractory Metals & Hard Materials 26 (2008) 601–605.
[23] S.K. Bhaumik, G.S. Upadhyaya, M.L. Vaidya, Full density processing of complex WC-based cemented carbides, Journal of Materials Processing Technology 58 (1996) 45–52.
[24] J.A. Arsecularatne, L.C. Zhang, C. Montross, Wear and tool life of tungsten carbide, PCBN and PCD cutting tools, International Journal of Machine Tools and Manufacture 46 (2006) 482–491.
[25] W. Bouzid, Cutting parameter optimization to minimize production time in high speed turning, Journal of Materials Processing Technology 161 (2005) 388–395.
[26] V.P. Astakhov, The assessment of cutting tool wear, International Journal of Machine Tools and Manufacture 44 (2004) 637–647.
[27] A.L.B. Dos Santos, M.A.V. Duarte, A.M. Abrão, A.R. Machado, An optimisation procedure to determine the coefficients of the extended Taylor's equation in machining, International Journal of Machine Tools and Manufacture 39 (1999) 17–31.
[28] I.E. Saklakoglu, N. Saklakoglu, V. Ceyhun, K.T. Short, G. Collins, The life of WC–Co cutting tools treated by plasma immersion ion Implantation, International Journal of Machine Tools and Manufacture 47 (2007) 715–719.
[29] J.X. Deng, W.L. Song, H. Zhang, J.L. Zhao, Performance of PVD MoS_2/Zr-coated carbide in cutting processes, International Journal of Machine Tools and Manufacture 48 (2008) 1546–1552.